16th International Conference on Integrated Modeling and Analysis in Applied Control and Automation
20th International Multidisciplinary Modeling & Simulation Multiconference

2724-0045 © 2023 The Authors.
doi: 10.46354/i3m.2023.mas.015

Simultaneous occurrence of intermittent and incipient faults

W. Borutzky[1,*]

[1]Bonn-Rhein-Sieg University of Applied Sciences, Sankt Augustin, Germany

[*]W. Borutzky. wolfgang.borutzky@h-brs.de

Abstract

Diagnosis and prognosis of intermittent faults, in general, is difficult as it is unknown when and for how long intermittent faults will reappear. This paper addresses the case of parametric incipient faults and simultaneously occurring intermittent faults with a magnitude that increases over time so that they may reach a failure alarm threshold and may eventually lead to a component or even a system failure.
The presented Bond Graph-based approach consists of two parts. First, a Diagnostic Bond Graph (DBG) is developed offline for an online diagnosis of intermittent faults by means of Analytical Redundancy Relations (ARRs). Due to the magnitude of intermittent faults increasing with time, the time evolutions of ARRs indicate a degradation trend. In a second, data-based, part, values of this trend over a moving time window stored in a buffer are extrapolated concurrently to the monitoring and to the fault detection and isolation (FDI) part in a repeated failure prognosis resulting in a sequence of Remaining Useful Life (RUL) estimates. A case study considers a small switched electronic circuit.

Keywords: Intermittent faults, Parametric incipient faults, Diagnostic Bond Graph, Fault diagnosis, Concurrent repeated failure prognosis.

1. Introduction

Failure prognostic is an essential part of Prognostic and Health Management (PHM) for all safety critical engineering systems and processes, for supervision, automation and condition based maintenance (CBM) of industrial processes and, clearly requires detection, isolation and estimation of faults. Data-driven as well as physics model-based approaches to Fault Detection and Isolation (FDI) are widely used in industry and in academia, see, for instance, Blanke et al. (2006); Tanwani et al. (2011); Escobet et al. (2014); Gao et al. (2015).

Elaborated presentations of bond graph model-based FDI may be found in books such as Samantaray and Ould Bouamama (2008); Wang et al. (2013); Borutzky (2015). FDI has mostly addressed abrupt as well as incipient faults. In recent years, research has extended to FDI of intermittent faults, see, for instance, Syed W. et al. (2016).

More recently, combinations of model-based and data-driven approaches have also been used for failure prognosis. In comparison to fault diagnosis, combined model-based and data-driven failure prognosis is still a subject of ongoing research. A 2016 survey on failure prognostic may be found in Elattar, H. M. et al. (2016). Combined bond graph model-based, data-driven approaches have been presented in Jha et al. (2017); Borutzky (2019, 2020).

Failure prognosis has mostly considered the case of incipient parametric faults because a degradation trend can be extracted from measurements in a moving time window and can be projected into the future in order to obtain estimates of the remaining useful life (RUL). In contrast, inci-

© 2023 The Authors. This article is an open access article distributed under the terms and conditions of the Creative Commons Attribution (CC BY-NC-ND) license (https://creativecommons.org/licenses/by-nc-nd/4.0/).

dents of intermittent faults, their duration and their magnitude are unpredictable. So far, jointly performed fault diagnosis and failure prognosis of intermittent faults has been addressed in a rather small number of publications, for instance, in Ming Yu et al. (2020); Borutzky (2023).

This paper considers the case of fault diagnosis and failure prognosis of intermittent and incipient parametric faults occurring simultaneously and is organised as follows:

The next section explains the fault diagnosis part of the approach based on an offline developed diagnostic bond graph (DBG). The fault diagnosis part cooperates with the failure prognosis part concurrently to the monitoring of a system.

The repeated failure prognosis part cooperating with the fault diagnosis part is addressed in Section 3.

In Section 4, intermittent fault diagnosis by means of Analytical Redundancy Relations (ARRs) and a repeated RUL estimation for intermittent faults is illustrated in a case study of an electronic circuit in which the power supply is subject to intermittent faults and a capacitor is leaking.

Section 4.3 shows that the approach is also applicable to sensors subject to intermittent faults.

Finally, Section 4.4 considers the case of incipient faults occurring simultaneously to intermittent faults by assuming that a capacitor in the electronic circuit is leaking.

The conclusion emphasises that intermittent faults are common in electronic interconnection systems and suggests the application of the presented BG model-based fault diagnosis approach combined with the data-based failure prognosis approach to further electronic systems with potential contact problems.

2. Fault diagnosis

The fault diagnosis part is performed concurrently to the monitoring of a process on an offline developed diagnostic bond graph (DBG) by numerically evaluating Analytical Redundancy Relations (ARRs) derived from the DBG. Numerical evaluation of ARRs results in residuals that serve as fault indicators. ARRs may be nonlinear dynamic equations and may even depend on discrete switch states in the case of switched models. The dependencies of ARRs from system parameters are usually captured in a structural fault signature matrix (FSM), which enables a direct detection of faults. If a fault signature is unique, a potentially faulty parameter can be isolated by inspection. In the case of multiple elements with the same fault signature, numerical parameter estimation can be used to identify the parameters that deviate from their nominal values. Once a faulty parameter has been isolated, the magnitude of a fault can be estimated at each next time instant in a sliding time window. Recording the obtained values reveals an unknown faulty time behaviour without the need of a mathematical model for the degradation trend, which might be difficult from physical first principles. In the offline simulation study in Section 4, the time evolution of the unstable power supply of a small electronic circuit subject to intermittent faults of increasing magnitude is reconstructed. At the same time a leaking capacitor develops an incipient parametric fault. The degradation trend of faults is reflected by the developing time evolution of ARR residuals as time proceeds. Extrapolations of residuals can be used to obtain a sequence of RUL estimates.

3. Concurrent repeated failure prognosis

The second part of the proposed approach uses the ARR residuals obtained in the first part for a repeated failure prognosis performed concurrently to the fault diagnosis. Once online fault diagnosis has resulted in a residual different from zero, system monitoring has to proceed until the residual value returns to zero before one can conclude that an intermittent fault happened. If, instead, the residual retains the nonzero value for quite some time, one may conclude that an abrupt fault happened. In case the residual returns to zero at some later time instant, it is clear that an intermittent fault of unforeseeable length has happened. Moreover, even when the residual under consideration returns to zero, one cannot be sure that another event of an intermittent fault will take place at any time instant later. Therefore, to be able to identify some degradation trend and to predict a RUL estimate, two consecutive intermittent faults must be detected and the latter one must be of higher fault magnitude. An estimate of a RUL may be obtained from a reconstructed fault signal by determining the intersection of an interpolation line through the points where the length of two consecutive intermittent faults end with an alarm threshold. The time point t_i is the time instant where a considered residual returns to zero.

If subsequent intermittent faults happen while time moves on, the process can be repeated. The result then is a sequence of RUL estimates that converges to zero with ongoing time. If the monotonic increase of intermittent fault magnitudes stops at some time instant, then RUL prediction is no longer possible but can resume when intermittent fault magnitudes increase again. As long as there is no intersection of an interpolating line with an alarm threshold no action is required and a system may continue its operation. On the contrary, time intervals between two consecutive intermittent faults may become shorter, their number may increase and may result in a permanent fault.

The approach to a repeated failure prognosis starting from ARR residuals obtained from a diagnostic BG is illustrated in Section 4 by means of an offline simulation. However, the diagnosis of intermittent faults as well as the simultaneous delayed extrapolation of fault values and the repeated RUL prediction can be performed online concurrently to the monitoring of the dynamic behaviour of a system.

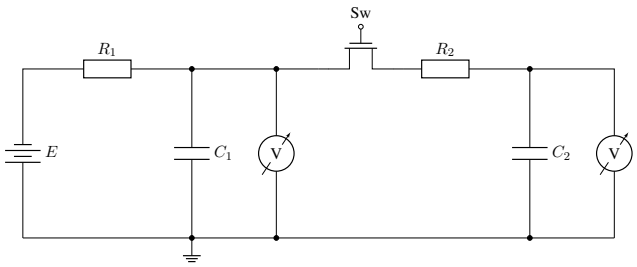

Figure 1. Simple switched circuit with two voltage sensors

Table 1. Parameters of the switched circuit in Fig. 1

Parameter	Value	Units	Meaning
E	5	V	Voltage supply
E_{thr}	1	V	Fault threshold
R_1	500	Ω	Resistor R : R_1
R_2	5	$k\Omega$	Resistor R : R_2
R_{on}	0.1	Ω	ON resistance of switch of Sw
C_1	5000	μF	Capacitor C : C_1
C_2	1000	μF	Capacitor C : C_2
$C_{2_{\text{crit}}}$	400	μF	Fault threshold
t_{sw}	10	s	Switching point of Sw
t_0	5	s	Start of the decay of $\tilde{C}_2(t)$
λ	0.0308065	s^{-1}	Rate of the decay

4. Intermittent and incipient parameter faults occurring simultaneously

The approach to a detection of simultaneous intermittent and incipient parametric faults and a repeated prediction of RUL estimates is illustrated by means of the simple electronic circuit in Fig. 1.

In this study, the real circuit is replaced by a BG model and offline simulation is performed that uses the parameter in Table 1.

It is assumed that the element parameters do not become faulty over time but keep their nominal value except the power supply $E(t)$ and the capacitance C_2.

To obtain pseudo measurements, the time evolution of the voltages numerically computed by means of the open source simulation program `Scilab` Scilab Team, ESI Group (2020) are overlayed with noise. These 'measurements' are filtered before they are input into the DBG for the computation of ARRs.

```
tu1n = tu1+ 0.02* tu1 .* rand(tu1,"normal");    (1)
```

In (1), the tilde denoting measurements from the faulty system, is replaced by the preceding letter `t`; the suffixed letter 'n' indicates that the net signal is overlayed with noise.

Figure 2 depicts the noisy measurements $\tilde{u}_1, \tilde{u}_2$ of the capacitor voltages. They are smoothed by the `Scilab` function `lsq_splin()`.

Fig. 3 shows the time evolutions of the smoothed capacitor voltages $\tilde{u}_1, \tilde{u}_2$. Fig. 4 displays the time evolution of the smoothed voltage $\tilde{u}_1$ together with its time derivative $\dot{\tilde{u}}_1$.

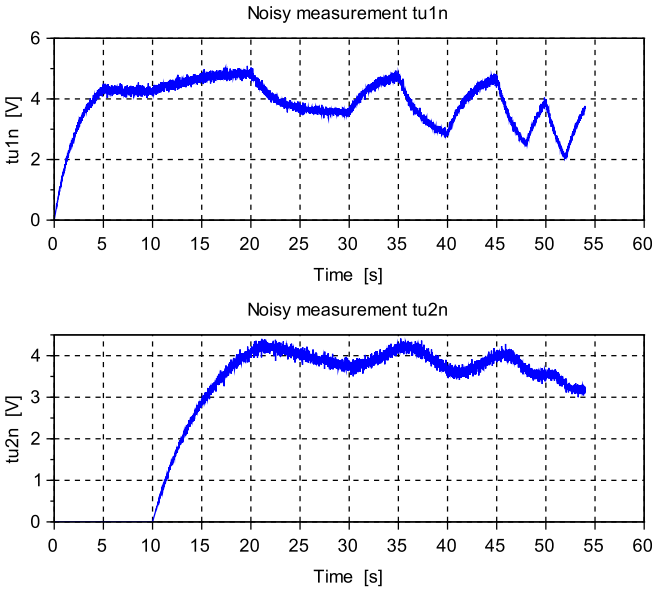

Figure 2. Time evolutions of the noisy capacitor voltages $\tilde{u}_1, \tilde{u}_2$

4.1. Intermittent fault diagnosis

Fig. 5 depicts the DBG of the circuit, in which the voltages with a tilde denote measurements from the faulty system. It is assumed that the voltage sensors themselves presented by the detectors De : $\tilde{u}_1$ and De : $\tilde{u}_2$ are faultless.

From the DBG in Fig. 5 the following two mode-dependent ARRs can be deduced.

$$\begin{aligned} \mathrm{o}_1 : \mathrm{ARR}_1 : \quad r_1 &= i_1 - i_{\text{sw}} - C_1\dot{\tilde{u}}_1 \\ &= \frac{E - \tilde{u}_1}{R_1} \\ &\quad - \frac{b^2}{R_{\text{on}} + b \cdot R_2}(\tilde{u}_1 - \tilde{u}_2) - C_1\dot{\tilde{u}}_1 \\ &= \frac{E - \tilde{u}_1}{R_1} - \frac{b}{R_2}(\tilde{u}_1 - \tilde{u}_2) - C_1\dot{\tilde{u}}_1 \end{aligned} \tag{2}$$

$$\mathrm{o}_2 : \mathrm{ARR}_2 : \quad r_2 = i_{\text{sw}} - C_2\dot{\tilde{u}}_2 = \frac{b}{R_2}(\tilde{u}_1 - \tilde{u}_2) - C_2\dot{\tilde{u}}_2, \tag{3}$$

where $b(t) \in \{0, 1\}$.

As can be seen from the structural fault signature matrix (FSM) (Table 2), none of the element parameters is isolatable, except C : C_2. Residual r_1 depends on elements R : R_1, C : C_1 and on R : R_2 in case the switch is closed. As a result, by inspection of the FSM it cannot be decided which parameter is faulty and causes an abnormal behaviour of the circuit. By means of parameter estimation over a time window it can be shown that the element parameters, in fact, do not deviate from their nominal values.

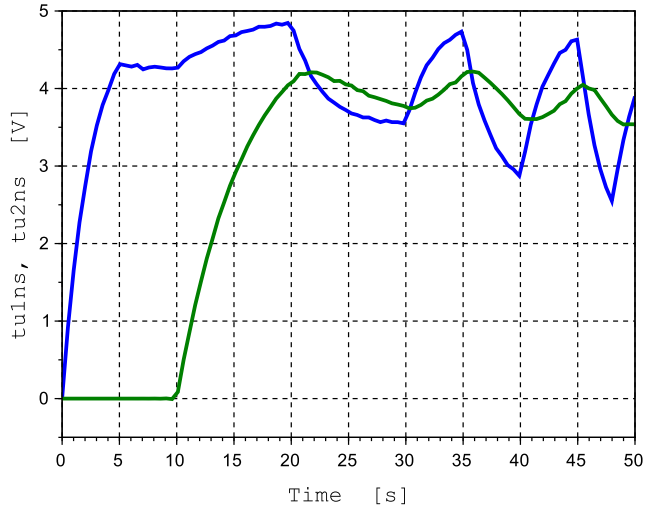

Figure 3. Time evolutions of the smoothed capacitor voltages $\tilde{u}_1, \tilde{u}_2$

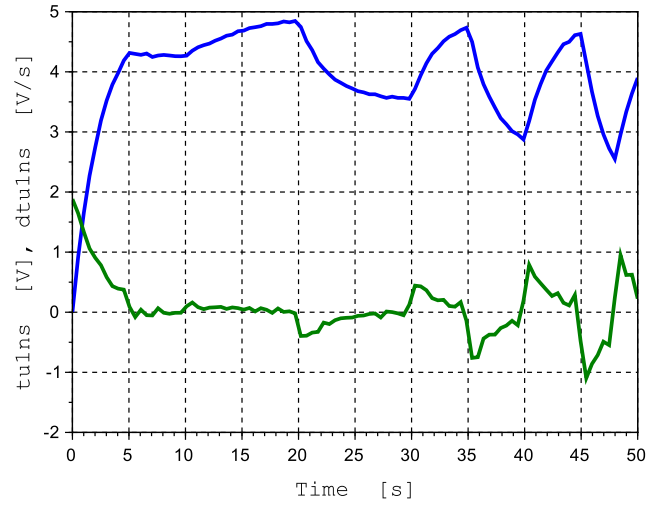

Figure 4. Time evolutions of the smoothed capacitor voltage $\tilde{u}_1$ and its time derivative $\dot{\tilde{u}}_1$

Numerical computation of (2) yields for the residual $\text{res}_1 = R_1 \cdot r_1$ a time evolution that clearly enables to detect the intermittent faults (Fig. 6). Residual res_1 can also be used to estimate the magnitude of the intermittent faults and to reconstruct the unknown faulty voltage supply $\tilde{E}$. If the constant voltage E in (2) is replaced by the faulty unknown one $\tilde{E}$, then ARR_1 reads:

$$0 = \frac{\tilde{E} - \tilde{u}_1}{R_1} - \frac{b}{R_2}(\tilde{u}_1 - \tilde{u}_2) - C_1\dot{\tilde{u}}_1 \tag{4}$$

Solving for $\tilde{E}$ and observing (2) gives

$$r\tilde{E} = E - R_1 r_1 = E - \text{res}_1 = \tilde{E} \tag{5}$$

$$\Delta E = \text{res}_1 \tag{6}$$

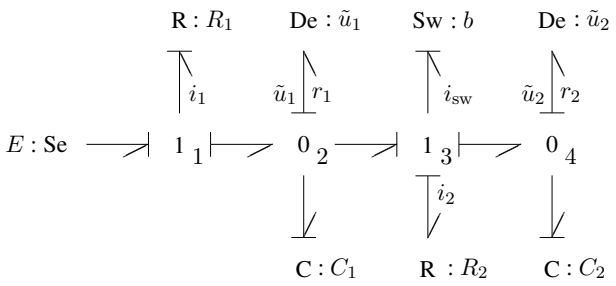

Figure 5. Diagnostic bond graph of the circuit in Fig. 1

Table 2. Structural FSM for the switched network in Fig. 1

Element	Parameter	r_1	r_2	D_b	I_b
Voltage source	E	1	0	1	0
De : $\tilde{u}_1$	$\tilde{u}_1$	1	1	1	0
De : $\tilde{u}_2$	$\tilde{u}_2$	1	1	1	0
Switch	b	b	b	b	0
R : R_1	R_1	1	0	1	0
R : R_2	R_2	b	b	b	b
C : C_1	C_1	1	0	1	0
C : C_2	C_2	0	1	1	1

4.2. Repeated RUL estimation for intermittent faults

From Fig. 6 one can see that the intermittent faults return to zero at time instances $t = 10, 30, 40, 48\,s$. Connecting the values of the reconstructed time evolution of the faulty voltage supply $rE(t)$ at two consecutive time points yields lines that intersect with an alarm threshold defined to be $1\,V$ as depicted in Fig. 7.

The time points of the intersections with the alarm threshold yield the decrease of the RUL over time shown in Fig. 9. The offline simulation running up to $t = 50\,s$ takes into account that online measurement cannot look into the future. Measurements only available up to the current time instant can be used for computing ARR residuals and for reconstruction of a time behaviour subject to intermittent faults. Although the latest intermittent fault return to zero at $t = 48\,s$, we cannot be sure at that time point that another intermittent fault will follow.

As an alarm threshold is chosen well with a distance to the failure threshold, the faulty supply voltage can still cross the alarm threshold due to an intermittent fault without causing harm to the system. Let t_4 be the last time instant where $r\tilde{E}(t_4)$ still has a distance to the alarm threshold and where $r\tilde{E}$ returns to the constant value E and let t_f be the time point where $r\tilde{E}(t_f)$ touches or crosses the threshold for the first time. The last RUL value different from zero then reads $RUL(t_4) = t_f - t_4$ and $RUL(t_f) = 0$. Fig. 8 shows the case where the true faulty voltage crosses the alarm threshold due to the last intermittent fault. The last RUL value different from zero is $RUL(t_4 = 48\,s) = 2\,s$

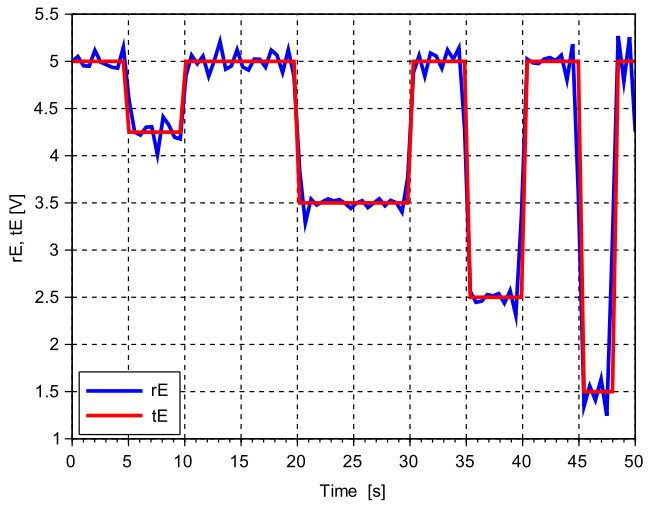

Figure 6. Reconstructed input voltage `rtE` and faulty input voltage `tE`

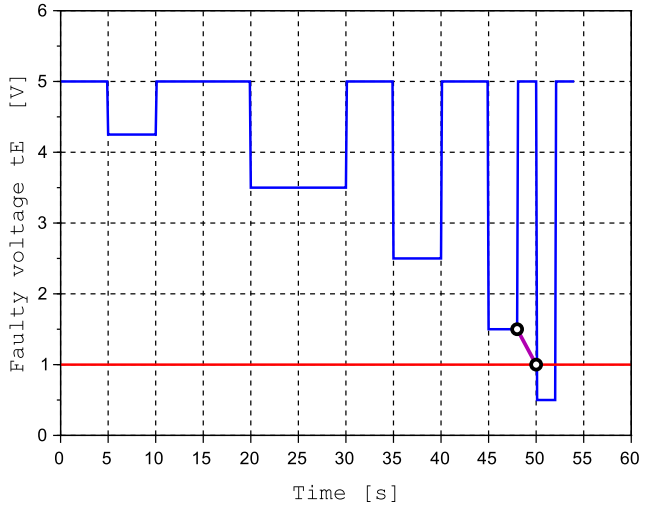

Figure 8. Determination of a last RUL value different from zero

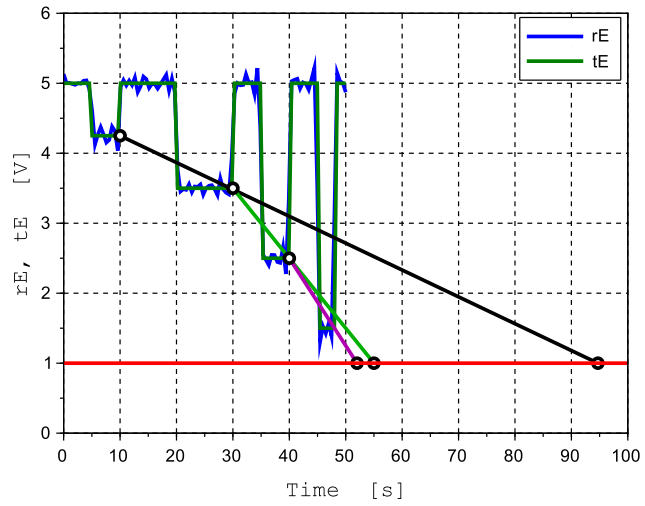

Figure 7. Repeated RUL estimation

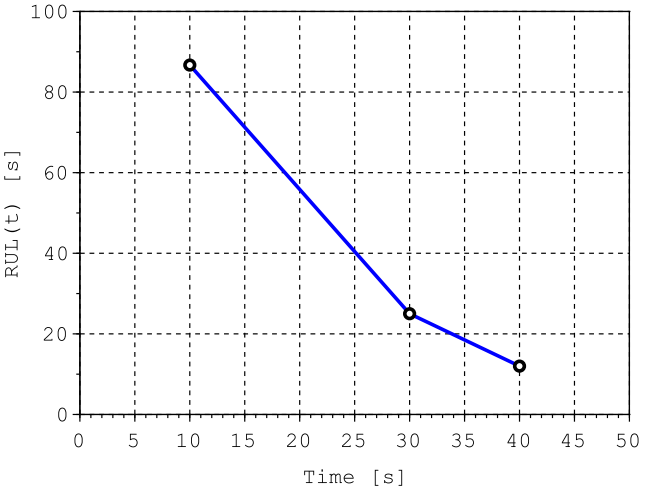

Figure 9. Decrease of the RUL over time

and t_f = 50 s.

4.3. Sensor subject to intermittent faults

Residuals derived from a DBG can also be used to detect a sensor with intermittent faults and to reconstruct the faultless signal. Let's assume that the circuit in Fig. 1 doesn't have any parametric faults. If the measurements of the capacitor voltages are correct then the residuals of ARRs (2), (3) are zero or close to zero. In contrast, if sensor De : $\tilde{u}_1'$ provides a faulty reading $\tilde{u}_1'(t)$ subject to intermittent faults due to connection problems then the residuals of both ARRs are different from zero. In the DBG in Fig. 10, the faulty reading $\tilde{u}_1'$ is highlighted in red.

Fig. 11 shows the true transient behaviour $u_1(t)$ and the faulty voltage $u_1'(t)$ which temporarily drops to zero due to contact problems. As noise is filtered anyway before measurements are used in the ARRs, noise has been neglected in Fig. 12.

Assume for simplicity that the second sensor De : $\tilde{u}_2$ provides faultless readings. ARR (3) then yields

$$0 = \frac{b}{R_2}(\tilde{u}_1 - \tilde{u}_2) - C_2\dot{\tilde{u}}_2 \tag{7}$$

$$r_2 = \frac{b}{R_2}(\tilde{u}_1' - \tilde{u}_2) - C_2\dot{\tilde{u}}_2 \tag{8}$$

Substraction of both equations gives for the reconstruction of the faultless signal $\tilde{u}_1(t)$

$$R_2 \cdot r_2 = b\,(\tilde{u}_1' - \tilde{u}_1) \tag{9}$$

or

$$r\tilde{u}_1 = \tilde{u}_1' - R_2 \cdot r_2 = \tilde{u}_1' - res_2 \tag{10}$$

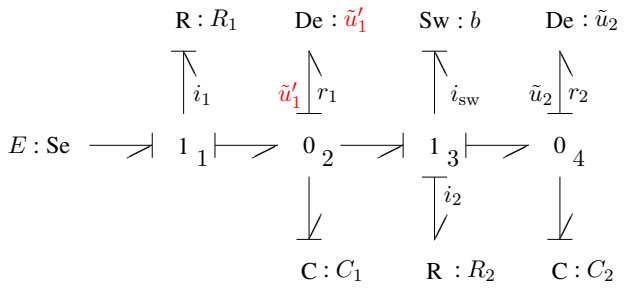

Figure 10. Diagnostic BG of Fig. 1 with a faulty input $u'_1(t)$

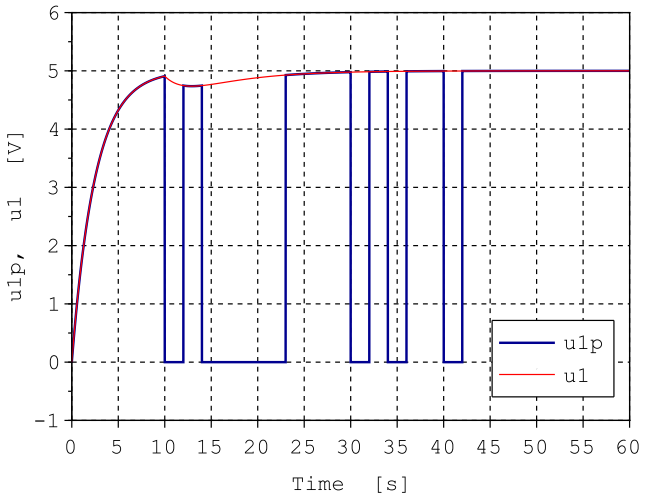

Figure 11. True transient behaviour of $u_1(t)$ and faulty reading $u'_1(t)$

for $t \geq t_{sw}$.

As can be seen from Fig. 12, the waveform of residual $res_2(t)$ complements the one of the faulty signal $\tilde{u}'_1(t)$ in the time intervals where the latter one drops to zero. The result of the overlay of both waveforms is just the reconstruction $r\tilde{u}_1(t)$ of the time history of the true capacitor voltage $\tilde{u}_1$.

The reconstruction $r\tilde{u}_1(t)$ can also be obtained from ARR 2. However, the computation of $r_1(t)$ requires the numerical differentiation of the faulty readings $\tilde{u}'_1$ with almost instantaneous drops to zero at unpredictable time instances.

$$r_1 = \frac{E - \tilde{u}'_1}{R_1} - \frac{b}{R_2}(\tilde{u}'_1 - \tilde{u}_2) - C_1\dot{\tilde{u}}'_1 \tag{11}$$

4.4. Leaking capacitor

In the following, it is assumed that in addition to the intermittent faults on the constant voltage supply E the capacitance C_2 is simultaneously leaking following an exponential decay.

$$\tilde{C}_2(t) = \begin{cases} C_2 & t \leq t_0 \\ \frac{1}{5}C_2\left(1 + 4e^{-\lambda(t-t_0)}\right) & t \geq t_0 \end{cases} \tag{12}$$

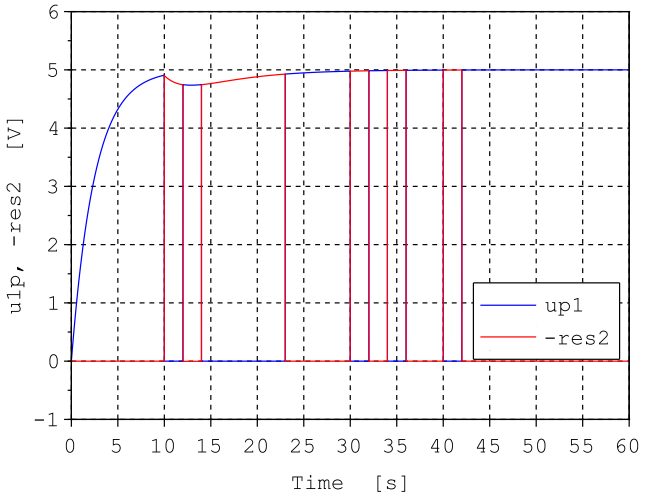

Figure 12. Reconstruction of $u_1(t)$ from faulty reading $u'_1(t)$ and residual $res_2(t)$

In the case of the simple example circuit in Fig. 1, the waveform of the faulty voltage $\tilde{E}(t)$ can be reconstructed from ARR_1. Independently, ARR_2 yields the degradation trend $\tilde{C}_2(t)$. Replacing the nominal capacitance C_2 in (3) by the unknown faulty time dependent capacitance $\tilde{C}_2(t)$ gives for the time evolution of $\tilde{C}_2(t)$.

$$0 = \frac{b}{R_2}(\tilde{u}_1 - \tilde{u}_2) - \tilde{C}_2(t)\dot{\tilde{u}}_2 \tag{13}$$

By subtracting (13) from (3) one obtains for the recovered faulty capacitance $r\tilde{C}_2(t)$

$$r\tilde{C}_2(t) = C_2 + \frac{r_2}{\dot{\tilde{u}}_2} \tag{14}$$

or

$$r\tilde{C}_2(t) = \frac{b}{R_2}\frac{\tilde{u}_1 - \tilde{u}_2}{\dot{\tilde{u}}_2} \tag{15}$$

Fig. 13 shows the waveforms of of smoothed capacitor voltages $\tilde{u}_1(t)$, $\tilde{u}_2(t)$ in the case C_2 is leaking in addition to the faulty voltage supply $\tilde{E}$

Clearly, recovery of the exponential decrease of capacitance C_2 from the voltage measurements can only start when the switch is closed for $t \geq t_{sw} = 10\ s$ ($b = 1$) and values $\tilde{u}_2(t)$ and $\dot{\tilde{u}}_2$ are available. Till that switching point, it is assumed that C_2 is faultless and keeps its nominal value. As Fig. 14 indicates, the true exponential decline $tC_2(t)$ actually starts earlier at $t = t_0 = 5\ s$ (Eq. 12).

The outliers on $rC2(t)$ can be removed or reduced by a moving median filter. The result $rC2m(t)$ is close to the true exponential decline $tC2(t)$ (Fig. 14).

Finally, in case an alarm threshold is set to be $C_{2_{crit}} = 0.4\ mF$, the time to reach this threshold would be $t_f = 50\ s$. Fig. 15 shows the RUL prediction for capacitance $rC2(t)$.

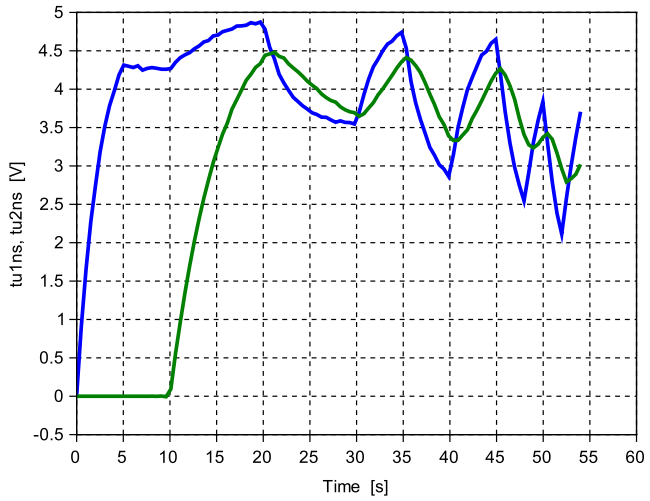

Figure 13. Time evolutions of smoothed capacitor voltages $\tilde{u}_1$,$\tilde{u}_2$ in the case C_2 is leaking in addition to a faulty voltage supply $\tilde{E}$

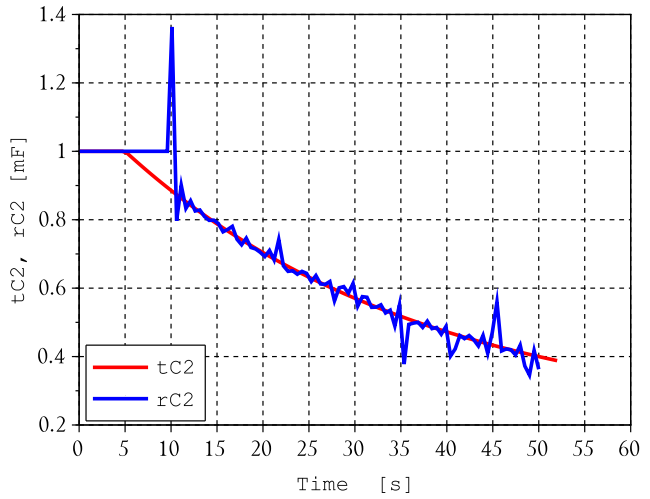

Figure 14. Recovered leaking capacitance $rC2(t)$

The degradation trend of the voltage supply due to intermittent faults of increasing magnitude reaches its lowest admissible values of 1 V also at t_f = 50 s (Fig. 8). Hence, the circuit's end of life (EoL) is 50 s. Clearly, for systems with faulty components the one with the fastest degradation trend determines the system's EoL.

5. Conclusion

The paper presents a BG model-based approach to diagnosis and failure prognosis of simultaneously occurring intermittent faults with a magnitude increasing over time and incipient parametric faults.

Faults are detected and estimated by evaluating ARRs derived from an offline developed DBG. Inputs into the DBG are known input signals and system measurements. Failure prognosis is done by repeated extrapolation of measurements.

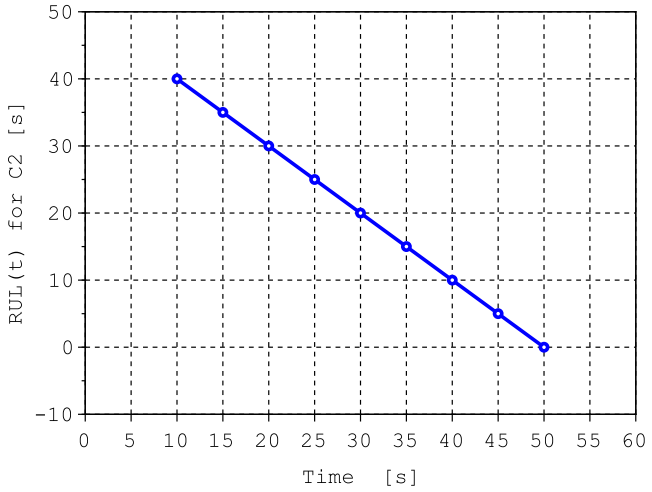

Figure 15. RUL prediction

Switching components can interrupt a prognosis concurrently performed to the monitoring of a system since in some system modes some measurements are not available. Clearly, the degradation trend of capacitance C_2 can only be extracted from measurements when the switch modelling the pass transistor is closed and the measurement of $u_2(t)$ is available.

In this case study, parameter uncertainties have been disregarded. However, they can be well taken into account in an uncertain BG, in a BG in linear fractional transformation form (BG-LFT), or in an incremental BG. Kam (2001); Borutzky (2010).

Intermittent faults are common in electronic interconnection systems. The approach can be applied to further electronic systems in which contact problems due to corrosion, moisture, or vibration can lead to unwanted uncontrolled, unpredictable connections or disconnections for short time intervals affecting the dynamic behaviour of a system and perhaps its safety.

References

Blanke, M., Kinnaert, M., Lunze, J., and Staroswiecki, M. (2006). *Diagnosis and Fault-Tolerant Control*. Springer, Berlin.

Borutzky, W. (2010). *Bond Graph Methodology – Development and Analysis of Multidisciplinary Dynamic System Models*. Springer-Verlag, London, UK. ISBN : 978-1-84882-881-0.

Borutzky, W. (2015). *Bond Graph Model-based Fault Diagnosis of Hybrid Systems*. Springer International Publishing Switzerland.

Borutzky, W. (2019). A Combined Bond Graph-based – Data-based Approach to Failure Prognosis. In Bruzzone, A., Dauphin-Tanguy, G., and Junco, S., editors, *Proc. 12h International Conference on Integrated Modelling and Analysis in Applied Control and Automation (IMAACA*

2019), part of the I3M Multiconference, pages 1 – 10, Lisbon, Portugal.

Borutzky, W. (2020). *Bond Graph Modelling for Control, Fault Diagnosis and Failure Prognosis*. Springer International Publishing Switzerland.

Borutzky, W. (2023). Diagnosis and Failure Prognosis of Intermittent Faults: A Bond Graph Approach. In Theilliol., D., Korbicz, J., and Kacprzyk, J., editors, *Recent Developments in Model-based and Data-driven Methods for Advanced Control and Diagnosis*, Book Series: Studies in Systems, Decision and Control. Springer Nature, Cham, Switzerland.

Elattar, H. M., Elminir, H. K., and Riad, A. M. (2016). Prognostics: a literature review. *Complex Intell. Syst.*, (2016) 2:125 – 154. open access.

Escobet, T., Puig, V., Quevedo, J., and Garcia, D. (2014). A methodology for incipient fault detection. In *2014 IEEE Conference on Control Applications (CCA)*, pages 104 – 109, Juan Les Antibes, France. IEEE.

Gao, Z., Cecati, C., and Ding, S. X. (2015). A Survey of Fault Diagnosis and Fault-Tolerant Techniques – Part I: Fault Diagnosis With Model-Based and Signal-Based Approaches. *IEEE TRANSACTIONS ON INDUSTRIAL ELECTRONICS*, 62(6):3757 – 3767.

Jha, M., Dauphin-Tanguy, G., and Ould Bouamama, B. (2017). Particle Filter Based Integrated Health Monitoring in Bond Graph Framework. In Borutzky, W., editor, *Bond Graphs for Modelling, Control and Fault Diagnosis of Engineering Systems*, pages 233–270. Springer International Publishing Switzerland.

Kam, C. (2001). *Les bond graphs pour la modélisation des systèmes linéaires incertains*. PhD thesis, L'Ecole Centrale de Lille et L'Université des Sciences et Technologies de Lille, Lille, France.

Ming Yu, Haotan Lu, Hai Wang, Chenyu Xiao, and Dun Lan (2020). Compound Fault Diagnosis and Sequential Prognosis for Electric Scooter with Uncertainties. *Acuators*, 9(128). doi:10.3390/act9040128, open access.

Samantaray, A. and Ould Bouamama, B. (2008). *Model-based Process Supervision – A Bond Graph Approach*. Advances in Industrial Control. Springer, London.

Scilab Team, ESI Group (2020). Scilab.

Syed W., Perinpanayagam S., Samie M., and Jennions I. (2016). A Novel Intermittent Fault Detection Algorithm and Health Monitoring for Electronic Interconnections. *IEEE Transactions on Components, Packaging and Manufacturing Technology*, 6(3):400–406. DOI: 10.1109/TCPMT.2015.2500023.

Tanwani, A., Domínguez-García, A., and Liberzon, D. (2011). An Inversion-Based Approach to Fault Detection and Isolation in Switching Electrical Networks. *IEEE Trans. on Control Systems Technology*, 19(5):1059–1074.

Wang, D., Yu, M., Low, C., and Arogeti, S. (2013). *Model-based Health Monitoring of Hybrid Systems*. Springer.